

# **Design and Synthesis of Small Molecule Inhibitors as Antimalarial Agents**

**M.Sc. Thesis**

By  
**Manisha Verma**



**DEPARTMENT OF CHEMISTRY  
INDIAN INSTITUTE OF TECHNOLOGY INDORE  
JUNE 2021**



# Design and Synthesis of Small Molecule Inhibitors as Antimalarial Agents

**A THESIS**

*Submitted in partial fulfillment of the  
requirements for the award of the degree  
of*  
**Master of Science**

*By*  
**Manisha Verma**



**DEPARTMENT OF CHEMISTRY  
INDIAN INSTITUTE OF TECHNOLOGY INDORE  
JUNE 2021**





# INDIAN INSTITUTE OF TECHNOLOGY INDORE

## CANDIDATE'S DECLARATION

I hereby certify that the work which is being presented in the thesis entitled **Design and Synthesis of Small Molecule Inhibitors as Antimalarial Agents** in the partial fulfillment of the requirements for the award of the degree of **MASTER OF SCIENCE** and submitted in the **DEPARTMENT OF CHEMISTRY, Indian Institute of Technology Indore**, is an authentic record of my own work carried out during the period from July 2020 to June 2021 under the supervision of Dr. Venkatesh Chelvam, Associate Professor, IIT Indore.

The matter presented in this thesis has not been submitted by me for the award of any other degree of this or any other institute.

*Manisha Verma*  
04-06-2021

**Manisha Verma**

---

This is to certify that the above statement made by the candidate is correct to the best of my knowledge.

**Dr. Venkatesh Chelvam**

---

**Manisha Verma** has successfully given her M.Sc. Oral Examination held on **June 09, 2021**

*Venkatesh.c*

Signature of Supervisor of M.Sc. thesis

**Dr. Venkatesh Chelvam**

Date: 9.6.2021

Convener, DPGC

**Dr. Tushar Kanti Mukherjee**

Date:

Signature of PSPC Member

**Dr. Sanjay Kumar Singh**

Date: 09.06.2021

Signature of PSPC Member

**Dr. Selvakumar Sermadurai**

Date: 09.06.2021

---



## ACKNOWLEDGEMENTS

It would be my great pleasure to offer appreciation to **Dr. Venkatesh Chelvam** for his great guidance and valuable suggestion throughout this whole course. His efforts were the fuel to my work that happened so smoothly. Under his excellent supervision, experience and advice, I was able to overcome all the obstacles that I faced during my M.Sc. project.

I am very grateful to Prof. Neelesh Kumar Jain (Officiating Director, Indian Institute of Technology, Indore) for his unending encouragement and providing all the facilities at Indian Institute of Technology Indore.

I would like to give my sincere thanks to the Department of Chemistry for providing me with the opportunity to pursue my M.Sc. Project.

I would like to sincerely thank my PSPC members **Dr. Sanjay Kumar Singh** and **Dr. Selvakumar Sermadurai** and **Dr. Biswarup Pathak** (Head, Department of Chemistry).

I thank profusely my lab members Dr. Amit Pandit, Dr. Mena Asha Krishnan and Ms. Kratika Yadav. With their support and constant effort, I was able to conduct my work quite easily and confidently.

I am thankful to the technical staff of Sophisticated Instrumentation Centre (SIC), IIT Indore Mr. Kinny Pandey, Mr. Ghanshyam Bhavsar and Chemistry Office staff Mr. Manish Kushwaha, Mr. Parthiban, Mr. Rameshwar Dohare and Ms. Vinita Kothari for their help and support.

I need to express my deepest love and gratitude to my lovable father Mr. Shyoji Ram Bairwa and to my lovable mother Mrs. Suman Devi and my sister Mrs. Monika Verma and my friends Mr. Durgesh Sarothiya and Mr. Naveen Somani for their unconditional love with their relentless support, unending encouragement and patience during this tenure.

Finally, I would like to acknowledge IIT Indore for providing infrastructure and all the facilities needed to carry out my research work efficiently and smoothly.

Manisha Verma



***DEDICATED TO MY LOVABLE  
FAMILY, FRIENDS AND  
TEACHERS.....***



## Abstract

Malaria has been a global issue for the last two decades and resulted in 409,000 deaths and 229 million cases in 2019 by *Plasmodium falciparum* (Pf) species alone. Dihydropteroate synthetase (DHPS) and Dihydrofolate reductase (DHFR) acts as promising targets for antimalarial drug candidates. We have designed different heterocyclic cores as small molecule inhibitors for *Pf*DHFR and *Pf*DHPS proteins. Initially, single-target therapy was used for the treatment of malaria but as resistant strains emerged, it was replaced by combination therapy using multiple drugs to overcome the resistance and these combination drugs show high synergistic effect. By using protein crystal data and molecular docking studies we determined the optimal interactions of inhibitors to explore the binding modes and binding affinities to the active site. In this project we try to design and synthesize compounds, having better activity towards resistant strains and exhibit low cytotoxicity, which can be further developed as promising antimalarial drugs.

In this work, we have reported two step syntheses that can be used for the gram scale synthesis of sulfonamides. We started our synthesis using naturally occurring L-amino acids as the chiral source and successfully synthesized intermediates which can be used for furnishing the final sulfonamide products. All the intermediates are well characterized using various spectroscopic techniques.

# TABLE OF CONTENTS

|   |                 |
|---|-----------------|
| <b>LIST OF FIGURES</b>  | <b>ix</b>       |
| <b>LISTS OF SCHEMES</b>   | <b>x</b>        |
| <b>LIST OF TABLES</b>   | <b>xi</b>       |
| <b>SYMBOLS/UNITS</b>  | <b>xii</b>      |
| <b>ACRONYMS</b>   | <b>xiii-xiv</b> |
| <b>Chapter 1: Introduction</b>  | <b>1-6</b>      |
| 1.1 Statistics of malaria across the world and in India   | 1               |
| 1.2 Enzymes involved in the synthesis of nucleic acids in malarial parasites                          | 2               |
| 1.2.1 <i>Plasmodium falciparum</i> dihydrofolate reductase PfDHFR                                     | 2               |
| 1.2.2 <i>Plamsodium falciparum</i> dihydropteroate synthetase PfDHPS                                  | 2-3             |
| 1.3 Objectives of the project   | 3               |
| 1.4 Synthetic design of DHPS and DHFR inhibitors  | 3-4             |
| 1.4.1 Retrosynthesis of DHPS inhibitors, 1  | 3               |
| 1.4.2 Retrosynthesis of DHFR inhibitors, 2  | 3-4             |
| 1.4.3 Design strategy   | 4               |
| 1.5 Work Plan or Methodology  | 4-6             |
| 1.5.1 Proposed synthesis of sulfonamide based DHPS inhibitors 1a–d                                    | 4-5             |
| 1.5.2 Proposed synthesis of folate based DHFR inhibitors 2a–o   | 5-6             |
| <b>Chapter 2: Literature Review</b>   | <b>7-11</b>     |
| 2.1 Folic acid derivatives as dihydrofolate reductase (DHFR) inhibitors and their mechanism of action | 7-9             |
| 2.2 DHPS structure and mechanism  | 9-10            |
| 2.3 Sulfonamides  | 10-11           |
| <b>Chapter 3: Experimental Section</b>  | <b>13-17</b>    |
| 3.1 Molecular docking   | 13              |
| 3.2 Materials and methods   | 13-14           |

|  |              |
|--|--------------|
| <b>3.3</b> Synthesis of nitrobenzenesulfonamides                               | <b>14-17</b> |
| <b>3.3.1</b> Synthesis of ((4-nitrophenyl)sulfonyl)-L-tryptophan ( <b>5a</b> ) | <b>14</b>    |
| <b>3.3.2</b> Synthesis of ((4-nitrophenyl)sulfonyl)-L-histidine ( <b>5b</b> )  | <b>15</b>    |
| <b>3.3.3</b> Synthesis of ((4-nitrophenyl)sulfonyl)-L-asparagine ( <b>5c</b> ) | <b>16</b>    |
| <b>3.3.4</b> Synthesis of ((4-nitrophenyl)sulfonyl)-L-asparagine ( <b>5d</b> ) | <b>16-17</b> |
| <b>3.3.5</b> Synthesis of ((4-aminophenyl)sulfonyl)-L-tryptophan ( <b>1a</b> ) | <b>17</b>    |
| <b>Chapter 4: Results and Discussions</b>                                      | <b>19-28</b> |
| <b>4.1</b> DHFR inhibitor  | <b>19-22</b> |
| <b>4.2</b> DHPS inhibitor  | <b>23-26</b> |
| <b>4.3</b> Retrosynthetic analysis of sulfonamide derivatives                  | <b>27</b>    |
| <b>4.4</b> Synthesis of ((4-aminophenyl)sulfonyl)-L-tryptophan ( <b>1a</b> )   | <b>27-28</b> |
| <b>Chapter 5: Conclusion</b>   | <b>29</b>    |
| <b>APPENDIX A</b>  | <b>30</b>    |
| <b>REFERENCES</b>  | <b>31-33</b> |

## LIST OF FIGURES

|                   |  |           |
|-------------------|--|-----------|
| <b>Figure 1.</b>  | Structure of 4-aminobenzoic acid and folic acid  | <b>4</b>  |
| <b>Figure 2.</b>  | Schematic representation of the protonation of DHF to form THF and hydride transfer from NADPH   | <b>7</b>  |
| <b>Figure 3.</b>  | Structure of methotrexate and aminopterin  | <b>9</b>  |
| <b>Figure 4.</b>  | Catalytic mechanism of DHPS and formation of stable cation $S_N1$ intermediate $DHP^+$   | <b>10</b> |
| <b>Figure 5.</b>  | Designed structures of DHFR inhibitors <b>2a–o</b>   | <b>20</b> |
| <b>Figure 6.</b>  | Superimposed orientation of newly designed inhibitors ( <b>2a–o</b> ) at the active site of DHFR protein (PBD ID 4DPD)                       | <b>22</b> |
| <b>Figure 7.</b>  | The H-bonding interaction of inhibitor <b>2a</b> at the active site of DHFR protein  | <b>22</b> |
| <b>Figure 8.</b>  | Designed structures of DHPS inhibitors <b>1a–d</b> and <b>11–20</b>  | <b>24</b> |
| <b>Figure 9.</b>  | Superimposed orientation of newly designed DHPS inhibitors ( <b>1a–d</b> and <b>11–20</b> ) at the active site of DHPS protein (PBD IB 3TYE) | <b>26</b> |
| <b>Figure 10.</b> | The H-bonding interaction of inhibitor <b>1b</b> at the active site of DHPS protein  | <b>26</b> |
| <b>Figure 11.</b> | $^1H$ NMR spectrum of <b>5a</b> in methanol- $d_4$   | <b>30</b> |

## LIST OF SCHEMES

|                  |   |          |
|------------------|---|----------|
| <b>Scheme 1.</b> | Retrosynthetic analysis of DHPS inhibitors, <b>1</b>        | <b>3</b> |
| <b>Scheme 2.</b> | Retrosynthetic analysis of DHFR inhibitors, <b>2</b>        | <b>4</b> |
| <b>Scheme 3.</b> | Synthesis of sulfonamide based DHPS inhibitors, <b>1a–d</b> | <b>5</b> |
| <b>Scheme 4.</b> | Synthesis of folate based DHFR inhibitors, <b>2a–o</b>      | <b>6</b> |

## LIST OF TABLES

|                 |   |
|-----------------|---|
| <b>Table 1.</b> | Molecular docking score of designed DHFR inhibitors <b>21</b> |
|                 | <b>2</b> with co-crystallised ligand, DHF                     |
| <b>Table 2.</b> | Molecular docking score of designed DHPS inhibitors <b>25</b> |
|                 | <b>1a–d</b> and <b>11–20</b> with co-crystallised ligand, YTZ |

## SYMBOLS/UNITS

|          |                    |
|----------|--------------------|
| $\alpha$ | Alpha              |
| Å        | Angstrom           |
| $\beta$  | Beta               |
| J        | Coupling constant  |
| $\delta$ | Delta              |
| dd       | Doublet of doublet |
| g/mg     | Gram/Milligram     |
| Hz/MHz   | Hertz/Mega Hertz   |
| h        | Hour               |
| Mmol     | Millimole          |
| mL       | Milli litre        |
| mM       | Milli molar        |
| M        | Molar              |
| nM       | Nano molar         |
| ppm      | Parts per million  |
| $R_f$    | Retention Factor   |

## ACRONYMS

Abbreviations used for amino acids, substituents, reagents etc. are largely in accordance with the recommendations of the IUPAC-IUB commission on Biochemical Nomenclature, 1974, Pure and Applied Chemistry, 40, 315-331. All amino acids have L-configuration. Standard three letter coding is used for all amino acids. Additional abbreviations used in this thesis are listed below.

|                   |                              |
|-------------------|------------------------------|
| ACN               | Acetonitrile                 |
| Asn               | Asparagine                   |
| CDCl <sub>3</sub> | Deuterated Chloroform        |
| DNA               | Deoxyribonucleic acid        |
| dTMP              | Deoxythymidine monophosphate |
| DHF               | Dihydrofolate                |
| DHFR              | Dihydrofolate reductase      |
| DHPPP             | Dihydropterin pyrophosphate  |
| DHPS              | Dihydropteroate synthetase   |
| d                 | Doublet                      |
| EtOAc             | Ethyl acetate                |
| His               | Histidine                    |
| HCl               | Hydrochloric acid            |
| m                 | Multiplet                    |

|                                 |                                 |
|---------------------------------|---------------------------------|
| NMR                             | Nuclear Magnetic Resonance      |
| <i>p</i> ABA                    | <i>para</i> -Aminobenzoic acid  |
| Phe                             | Phenylalanine                   |
| <i>Pf</i>                       | <i>Plasmodium falciparum</i>    |
| KCl                             | Potassium chloride              |
| s                               | Singlet                         |
| Na <sub>2</sub> SO <sub>4</sub> | Sodium sulphate                 |
| SAR                             | Structure activity relationship |
| THF                             | Tetrahydrofolate                |
| TMS                             | Tetramethylsilane               |
| TLC                             | Thin Layer Chromatography       |
| TS                              | Thymidylate synthase            |
| t                               | Triplet                         |
| Trp                             | Tryptophan                      |
| UV                              | Ultra-Violet                    |
| H <sub>2</sub> O                | Water                           |

### Introduction

#### 1.1 Statistics of malaria across the world and in India

Malaria is a lethal infection caused by single-celled eukaryotic parasite *Plasmodium*. Malaria is spread by *Plasmodium* infected female anopheles mosquitoes. In the year 2019, there were an estimated 40,900 deaths and 229 million cases occurred due to *Plasmodium falciparum* and 6.4 million malaria cases by *Plasmodium vivax* in 2019 [1]. The children aged under five represents two-thirds of these incidences. The large number of mortality and morbidity caused by *Plasmodium falciparum* was treated globally by adopting artemisinin-based combination therapies (ACTs) which was approved by WHO for less severe malaria cases [2]. The occurrence of resistance to existing antimalarial drugs and therapies resulted in reduced binding affinities of drugs rendering them ineffective. The first case of drug resistance was identified in 2004 in Cambodia [3]. Hence, the need for development of novel antimalarials in an efficient and rational manner is crucial.

Out of the total malaria cases globally, almost 85% are reported in India and 18 African countries. India reported 8.4 million cases in 2017, but surprisingly 2.6 million fewer cases in 2018. In 2018, more than 85% of globally estimated malaria cases by *Plasmodium vivax* were in just 6 countries and India accounted for 47% of it. The multidrug resistant strains of *Plasmodium falciparum* cause major global health issues and spread rapidly from Cambodia to neighboring Southeast Asian countries like India and China. The exponential increase in multidrug resistance reinforced the urgent need for the development of new antimalarial agents against existing validated targets and search for novel targets.

## **1.2 Enzymes involved in the synthesis of nucleic acids in malarial parasites**

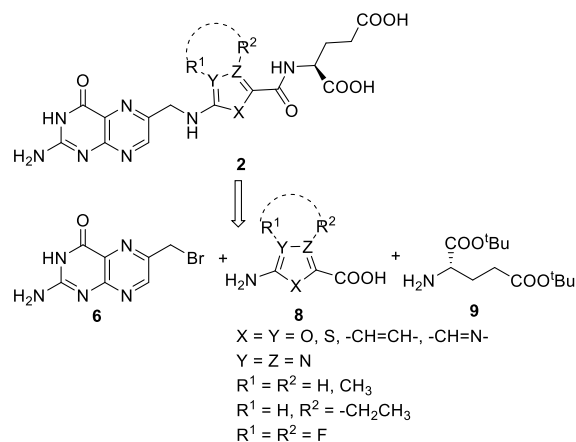
### **1.2.1 *Plasmodium falciparum* dihydrofolate reductase PfdHFR**

*PfdHFR*, an important enzyme in the folic acid synthesis pathway for the biosynthesis of amino acids and nucleic acids, DNA replication, and cell growth and essential for parasite survival. The enzyme catalyzes the reaction which reduces dihydrofolate to tetrahydrofolate. DHFR is encoded as the part of bifunctional enzyme along with thymidylate synthase (TS) in *Plasmodium falciparum* whereas it is present as two separate enzymes in human [4]. *PfdHFR*-TS is present in the form of dimer and each monomer contains 608 amino acid residues in length, having 231 residues in N-terminal DHFR domain and 288 residues in C-terminal TS domain. Both the domains are connected through a junction of 89 amino acids [5]. These structural data helps us to design selective, potent inhibitors and provide a scope of further antimalarial research.

### **1.2.2 *Plasmodium falciparum* dihydropteroate synthetase PfdHPS**

In protozoa, there is a *de novo* folate biosynthesis pathway unlike mammals which starts with the synthesis of dihydropteroate from dihydropterin pyrophosphate (DHPPP) and *para*-aminobenzoic acid (*pABA*) catalyzed by dihydropteroate synthetase (DHPS) enzyme. DHPS is a homodimer and is a target of many antimalarials agents like sulfonamides which are analogs of *pABA* [6]. The sulfonamide class of drugs targets *pABA* binding pocket. Initially DHPPP binds to the DHPS and then pyrophosphate is removed in a magnesium dependent reaction. After pyrophosphate elimination, *pABA* and pterin binding pockets open which allows for binding of *pABA* and pterin moieties to form dihydropteroate [7]. In *Plasmodium falciparum*, the enzyme is bifunctional and further catalyzes the addition of L-glutamate residue via gamma carboxylic acid to convert dihydropteroate to fully reduced folate species, dihydrofolate (DHF).





**Scheme 2.** Retrosynthetic analysis of DHFR inhibitors, **2**

### 1.4.3 Design strategy

The design strategy of the current project is based on the structural information of 4-amino benzoic acid and folic acid (Figure 1). The folate structure consists of pteridine ring, *p*-aminobenzoic acid (*p*ABA) and glutamic acid. Detailed study of *Pf*DHFR enzyme reaction was reported by Abbat *et al* to understand the binding affinity of *Pf*DHFR natural substrates, dihydrofolate (DHF). The modification of *p*ABA motif may mimic the natural substrate and act as a competitive inhibitor of DHPS and DHFR enzymes leading to potential antimalarial activity.

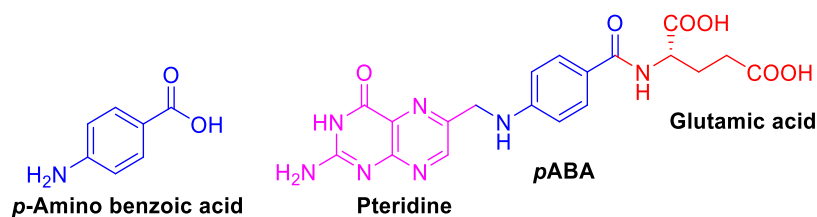


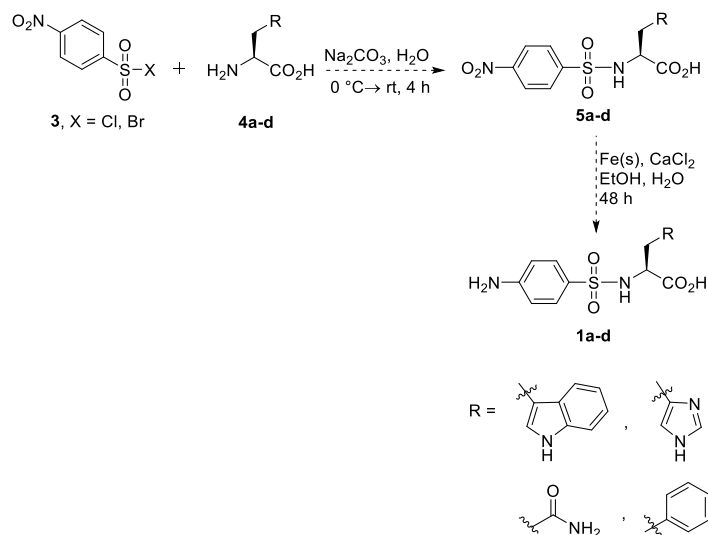
**Figure 1.** Structure of 4-amino benzoic acid and folic acid

## 1.5 Work Plan or Methodology

### 1.5.1 Proposed synthesis of sulfonamide based DHPS inhibitors 1a–d

4-Nitrobenzenesulfonyl chloride or bromide **3** reacts with L-amino acids **4a–d** in the presence of a base to form chiral sulfonamides **5a–d** which were

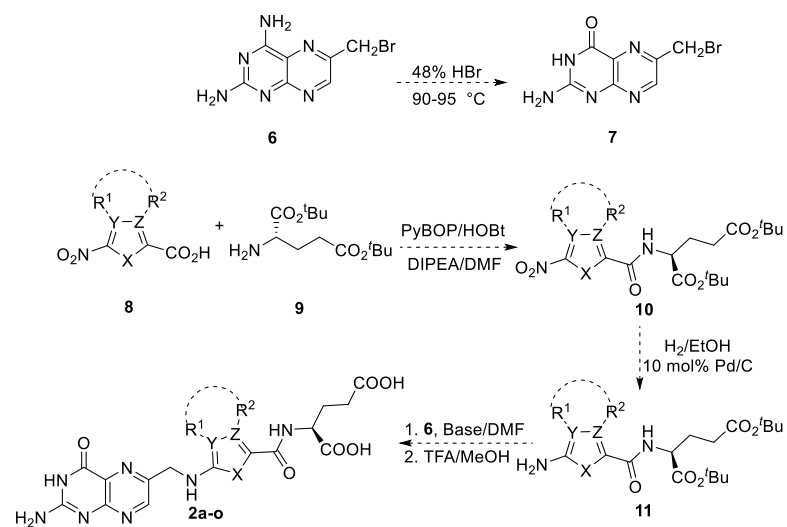
further reduced in the presence of iron powder and calcium chloride in aqueous ethanol to form chiral sulfonamides **1a–d** (Scheme 3).



**Scheme 3.** Proposed synthesis of sulfonamide based DHPS inhibitors **1a–d**

### 1.5.2 Proposed synthesis of folate based DHFR inhibitors **2a–o**

2,4-Diamino pteridine methyl bromide **6** undergo deamination reaction to form pteridine-2-methyl bromide **7** on reaction with hydrogen bromide at 95 °C. Meanwhile various substituted aromatic or heteroaromatic nitro acids of general structure **8** can be reacted with 1,3-*tert*-butylcarboxy-L-glutamic acid **9** in presence of coupling agent PyBOP to afford dipeptide **10** which can be converted to amino dipeptide **11** by palladium catalyzed hydrogenation in presence of H<sub>2</sub> gas. Amino dipeptide **11** can be reacted with pteridine-2-methyl bromide **7** to afford 1,3-*tert*-butylcarboxy protected folate derivatives. Finally, the *tert*-butylcarboxy protected folate derivatives can be deprotected under acidic condition using trifluoroacetic acid to form newly designed DHFR inhibitors **2a–o** (Scheme 4).



**Scheme 4.** Proposed synthesis of folate based DHFR inhibitors **2a-o**

## Review of past work

### 2.1 Folic acid derivatives as dihydrofolate reductase (DHFR) inhibitors and their mechanism of action

Folic acid is a form of water-soluble vitamin essential for biological systems and is a precursor of tetrahydrofolate (THF). Tetrahydrofolate is involved in the biosynthesis of amino acids, pyrimidines, purines and thymidylate (TM) and it is required for cell growth and proliferation hence it can be concluded that it is important for the basic functioning of the cell [8].

The two enzymes play important role in the synthesis of folates in the cells: dihydrofolate reductase (DHFR) and dihydrofolate synthase (DHPS). In cells, DHFR is required for reducing 7,8-dihydrofolate to 5,6,7,8-tetrahydrofolate with the help of NADPH cofactor (Figure 2). The key step in the mechanism of catalysis by DHFR is the protonation of dihydrofolate (DHF) to form tetrahydrofolate (THF) by the hydride ion transfer from nicotinamide adenine dinucleotide phosphate (NADPH) releasing  $\text{NADP}^+$ . NADPH transfers hydride ion from its C-4 position to the C-7 position of dihydrofolate [9, 10].

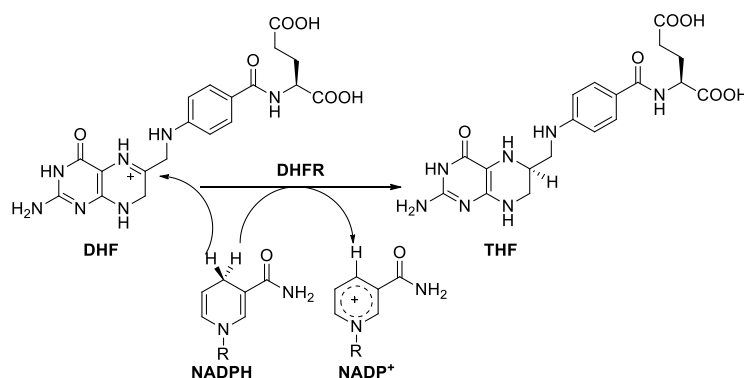


**Figure 2.** Schematic representation of the protonation of DHF to form THF via hydride transfer from NADPH

Dihydrofolate reductase is a small water-soluble protein having a molecular weight of 18000-25000 Da. The enzyme comprises of eight  $\beta$  sheets and four  $\alpha$ -helices responsible for connecting the  $\beta$  strands. The four loops of  $\alpha$ -helices are also involved in the formation of the binding pocket of the substrate and the coenzyme. DHFR contains no sulfide bridges and coordination with metal ions is not required to exercise its biochemical activity [11]. The substrate binds in the hydrophobic cleft located deeply in the enzyme and is surrounded by the  $\alpha$ -helix B, the central  $\beta$  sheets (a, e, and b), and the loop 1 [12].

The heterocyclic moiety containing folate molecules competitively bind with the active site of the enzyme by structurally mimicking natural substrate. The binding of inhibitors results in slow conformational change due to hydrogen bonding interactions with the amino acid residues present in the binding site of the enzyme.

Aminopterin and methotrexate are potent inhibitors of virtually all dihydrofolate reductase enzymes (Figure 3). Both have been proven to be potent inhibitors of *Plasmodium falciparum* growth during *in vitro* studies. Along with inhibiting parasitic growth, methotrexate also inhibits neoplastic cell division in the same concentration range. Because of high toxicity associated to the human host, the use of methotrexate is prohibited in several countries as antimalarial agents.

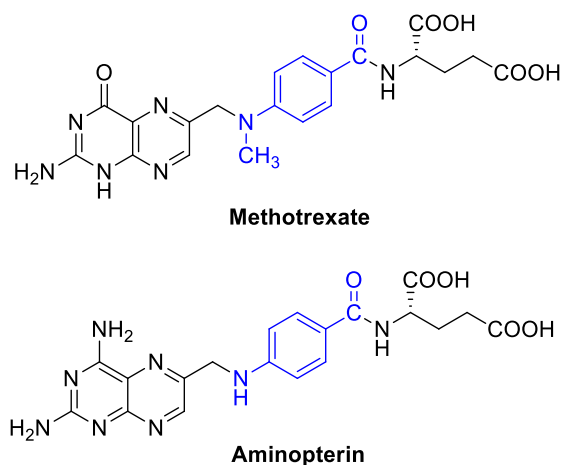


**Figure 3.** Structure of methotrexate and aminopterin

## 2.2 DHPS structure and mechanism

The structure of DHPS consists of eight  $\alpha$ -helices alternating with eight  $\beta$ -sheets and the active site is located at the ‘C-terminal’ end of the  $\beta$  barrel. The active site is composed of three sub-sites: the pterin-binding sub-site, the *p*ABA binding subsite and the anion-binding pocket. The pterin-binding pocket is located in the deep cleft at the center of the  $\beta$  barrel and involves many hydrogen-bonding interactions. The two flexible loops constitute the *p*ABA binding subsite and it binds with *p*ABA by hydrophobic and hydrogen-bonding interactions. The phosphate ion resides in the anion binding pocket and has a high affinity for binding. [13].

There are five key amino acid residues Asn 120, Asp 184, Lys 220, Arg 254, and His 256 which binds to the pterin-binding pocket and there are three amino acid residues Lys 220, Ser 218, Phe 189 which facilitate the hydrophobic interactions with the aromatic ring of *p*ABA and hydrogen bonding with the amine group. The *p*ABA binding pocket is a potential target and accommodates benzene-sulfonamide moiety in a better manner, leading to competitive inhibition of *p*ABA [14].

The catalytic mechanism of DHPS is illustrated in figure 4 which shows the condensation of DHPPP (dihydropterin pyrophosphate) and *p*ABA (*para*-

aminobenzoic acid) to form 7,8-dihydropteroate. The reaction proceeds through  $S_N1$  mechanism by binding of DHPPP with DHPS in the pterin-binding pocket accompanying the elimination of pyrophosphate (PPi) moiety forming cationic intermediate  $DHP^+$  whose resonance forms are indicated in the square brackets. The resonance forms are stabilized by delocalizing the positive charges into the pterin ring. The lone pairs on the amine group of the *p*ABA attacks at the C-9 carbon of the pterin ring of  $DHP^+$  intermediate to produce 7,8-dihydropteroate (DHP). The released pyrophosphate stabilizes the  $Mg^{2+}$  ion, loop 1 and loop 2. The  $Mg^{2+}$  ion orders the complex loop1-loop2 substructure which forms the binding pocket for *p*ABA [15, 16].

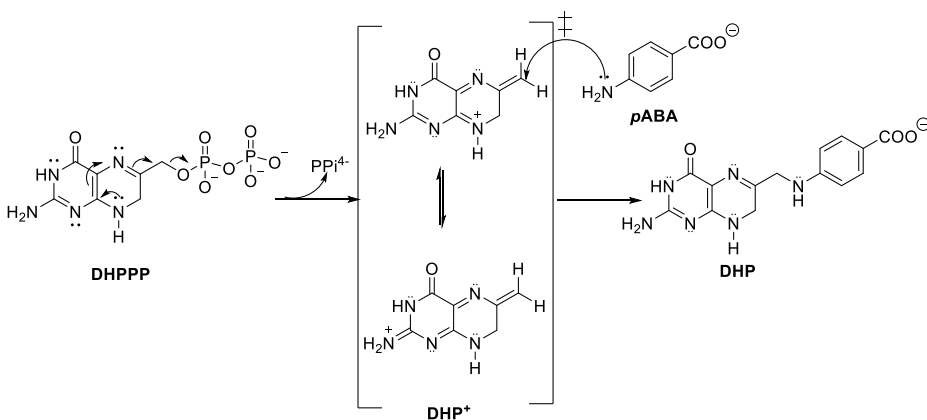


**Figure 4.** Catalytic mechanism of DHPS and formation of stable cationic  $S_N1$  intermediate  $DHP^+$

### 2.3 Sulfonamides

The sulfonamide based drugs were discovered from prontosil which gets metabolized to sulfanilamide (active ingredient for antibacterial activity) [17, 18]. After this discovery, analogs of sulfanilamides were synthesized and found to be potent synergizers of DHFR inhibitors. At present, dapsone, sulfadoxine, sulfalene are used as DHPS inhibitors for malaria.

The sulfonamide based drugs fit inside the *p*ABA binding pocket and the oxygen atom of the sulfonyl group shows interactions similar to those shown by the carboxyl group of *p*ABA and the phenyl group occupies the

hydrophobic pocket created by loop 1 and loop 2 [19]. Therefore, sulfonamides are close structure analogue of *p*ABA, and bind DHPS in a similar manner as natural substrate [20].

From recent literatures, it has been observed that drug resistance generally occurs when certain portions of the drugs extend beyond the molecular envelope [21]. It can be concluded that future DHPS inhibitors can be designed which do not extrude the active site and remain within the substrate envelope.



### Experimental Section

#### 3.1 Molecular Docking Study

The crystal structure of the target protein DHFR (PDB ID 4DPD) and DHPS (PDB ID 3TYE) were retrieved from the protein data bank. Newly designed two-dimensional ligand's structures were converted to three dimensions with the help of Chemoffice 2017. The protein and ligands were prepared as per the defined protocol and molecular docking study was performed by the Molegro virtual docker software (MVD, 6.0.0, CLC bio, Denmark, 2013).

#### 3.2 Material and Methods

All reagents were purchased from commercial suppliers like Spectrochem, Rankem, Loba Chemie, Alfa Aesar and were used without any further purification. All moisture sensitive reagents were stored in vacuum dessicator under inert atmosphere. To monitor the progress of the reactions, analytical thin layer chromatography (TLC) was performed on SiO<sub>2</sub> 60 F-254 plates. TLC plates were analysed under UV irradiation at 254 nm or by staining with ninhydrin, bromo cresol and iodine.

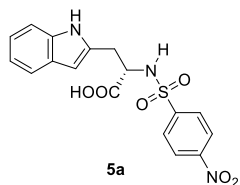
All volatile solvents were evaporated under appropriately reduced pressure at 40 °C using a rotary evaporator. All the synthesized compounds were purified by recrystallization using solvents through one-solvent or two-solvent crystallization techniques.

<sup>1</sup>H and <sup>13</sup>C NMR spectra were recorded using Bruker 500 MHz NMR spectrometer with trimethylsilane (TMS) as an internal reference. Deuterated solvents such as CD<sub>3</sub>OD and CDCl<sub>3</sub> were used as solvents for preparing the NMR sample. Chemical shift is reported in delta units and expressed in parts per million (ppm) downfield from TMS. Mass Spectra of

compounds dissolved in acetonitrile (ACN) and methanol were recorded on BRUKER DALTONICS Micro TOF-Q II mass spectrometer by positive and negative mode electrospray ionization method.

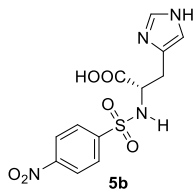
### 3.3 Synthesis of nitrobenzenesulfonamides

#### 3.3.1 Synthesis of ((4-nitrophenyl)sulfonyl)-L-tryptophan (**5a**)



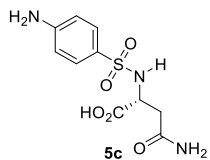
Sodium carbonate,  $\text{Na}_2\text{CO}_3$  (63 mg, 0.58 mmol) was added to a solution of L-tryptophan (100 mg, 0.48 mmol) in water (2 mL), in a 50 mL round bottomed flask and stirred for 20 minutes at room temperature. The solution was cooled to  $-5\text{ }^\circ\text{C}$  and 4-nitrobenzenesulfonyl chloride (130 mg, 0.58 mmol) was added portion-wise over a period of an hour. The reaction mixture was further stirred at room temperature for 24 h. After the complete consumption of the starting material (monitoring the progress by TLC), the reaction mixture was acidified using 20% aqueous HCl to pH 2. The solid product was filtered via suction and washed with pH 2.2 buffer (50 mL 0.2 M KCl and 7.8 mL 0.2 M HCl). The mixture was kept for recrystallization using ethanol to afford the product **5a** as a yellow solid (146 mg, 78%). TLC:  $R_f$  0.15 (1:9 MeOH/DCM).  $^1\text{H}$  NMR (400 MHz,  $\text{CD}_3\text{OD}$ )  $\delta$  : 7.77 (d,  $J = 8.7$  Hz, 2H), 7.45 (d,  $J = 8.7$  Hz, 2H), 7.28 (d,  $J = 7.6$  Hz, 1H), 7.03 (d,  $J = 8.0$  Hz, 1H), 6.95–6.87 (m, 2H), 4.11 (d,  $J = 10.4$  Hz, 1H), 3.23 (dd,  $J = 3.4$  Hz, 3.3 Hz, 1H), 2.90–2.84 (m, 2H) ppm.

### 3.3.2 Synthesis of ((4-nitrophenyl)sulfonyl)-L-histidine (**5b**)



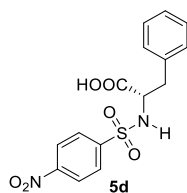
Sodium carbonate,  $\text{Na}_2\text{CO}_3$  (81.40 mg, 0.76 mmol) was added to a solution of L-histidine (100 mg, 0.64 mmol) in water (4 mL), in one neck 50 mL round bottomed flask and stirred for 20 minutes at room temperature. The solution was cooled to  $-5\text{ }^\circ\text{C}$  and 4-nitrobenzenesulfonyl chloride (170 mg, 0.76 mmol) was added portion-wise over a period of an hour. The reaction mixture was further stirred at room temperature for 72 h. After the complete consumption of the starting material (monitoring the progress by TLC), the reaction mixture was acidified using 20% aqueous HCl to pH 2. The aqueous layer was extracted using EtOAc ( $3 \times 15$  mL). The combined EtOAc layers were dried over  $\text{Na}_2\text{SO}_4$ , filtered and evaporated. The crude product thus obtained, was purified by recrystallization using ethanol and water (4:1) and the product **5b** was obtained as pale yellow solid (90 mg, 41%). TLC:  $R_f$  0.12 (2:8 MeOH/DCM).

### 3.3.3 Synthesis of ((4-nitrophenyl)sulfonyl)-L-asparagine (**5c**)



Sodium carbonate,  $\text{Na}_2\text{CO}_3$  (84 mg, 0.79 mmol) was added to a solution of L-asparagine (100 mg, 0.66 mmol) in water (4 mL), in one neck 50 mL round bottomed flask and stirred for 20 minutes at room temperature. The solution was cooled to  $-5\text{ }^\circ\text{C}$  and 4-nitrobenzenesulfonyl chloride (176 mg, 0.79 mmol) was added portion-wise over a period of an hour. The slurry was further stirred at room temperature for 72 h. After the complete consumption of the starting material (monitoring the progress by TLC), the mixture was filtered and concentrated. The solid product was purified through recrystallization using ethanol-water (4:1) by two-solvent recrystallization technique. The purified product **5c** was obtained as white crystalline solid (241 mg, 86%). TLC:  $R_f$  0.23 (1:9 MeOH/EtOAc).

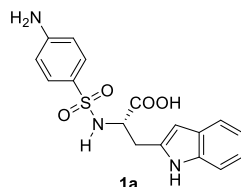
### 3.3.4 Synthesis of ((4-nitrophenyl)sulfonyl)-L-phenylalanine (**5d**)



Sodium carbonate,  $\text{Na}_2\text{CO}_3$  (77 mg, 0.72 mmol) was added to a solution of L-phenylalanine (100 mg, 0.60 mmol) in water (4 mL), in one-neck 50 mL round bottomed flask and stirred for 20 minutes at room temperature. The solution was cooled to  $-5\text{ }^\circ\text{C}$  and 4-nitrobenzenesulfonyl chloride (160 mg, 0.72 mmol) was added portion-wise over a period of an hour. The reaction mixture was further stirred at room temperature for 48 h. The progress of the reaction was monitored using TLC. After the complete consumption of the starting material, the pH of the reaction mixture was adjusted to 2 using 20% aqueous HCl. The crystals thus formed were filtered via suction

through vacuum filtration setup in the Buchner funnel and then dried. The pure product **5d** was obtained as a yellow solid (170 mg, 81%). TLC:  $R_f$  0.16 (1:9 MeOH/DCM).

### 3.3.5 Synthesis of ((4-aminophenyl)sulfonyl)-L-tryptophan (**1a**)



Nitrobenzenesulfonamide (100 mg, 0.25 mmol) was added in a mixture of ethanol (42 mg, 0.75 mmol), calcium chloride (28 mg, 0.25 mmol) and iron powder (41.86 mg, 0.75 mmol) in one neck 50 mL round bottomed flask. After mixing, the suspension was stirred at 60 °C for 30 minutes. The progress of the reaction was monitored through TLC for 48 h. After complete consumption of the starting material, the reaction mixture was filtered to remove the iron residues. The filtrate thus obtained was washed with EtOAc (2×10 mL). The organic extracts were washed with H<sub>2</sub>O (3×10 mL) and dried over anhydrous sodium sulfate. The organic layer was evaporated under reduced pressure using rotary evaporator and purified by recrystallization using 3:1 EtOH-H<sub>2</sub>O. The purified product was obtained as yellow-brown solid (193 mg, 47%). TLC:  $R_f$  0.18 (0.5:9.5 MeOH/EtOAc).



### Results and Discussions

#### 4.1 DHFR Inhibitor

The crystal structures of dihydrofolate reductase (DHFR) in PBD ID 4DPD is co-crystallised with inhibitor dihydrofolic acid (ID-DHF). The H-bonding interactions between the dihydrofolate (DHF) and amino acid residues of DHFR protein were analysed. Based on the study, various DHFR inhibitors were designed and screened through molecular docking analysis. The top scoring inhibitors (**2a–o**) are mentioned in figure 5. The molecular docking scores of the designed inhibitors are given in table 1. All the designed inhibitors interact at the active site in a similar way as that of DHF ligand. The superimposed orientations of all the ligands are mentioned in figure 6. Inhibitor **2a** has highest score among all the inhibitors and hence the H-bonding interaction of the inhibitor **2a** was evaluated in detail (Figure 7). All the designed inhibitors have shown significant interactions at the DHFR active site in *in silico* study. Synthesis and *in vitro* evaluation will be performed to validate the theoretical study.

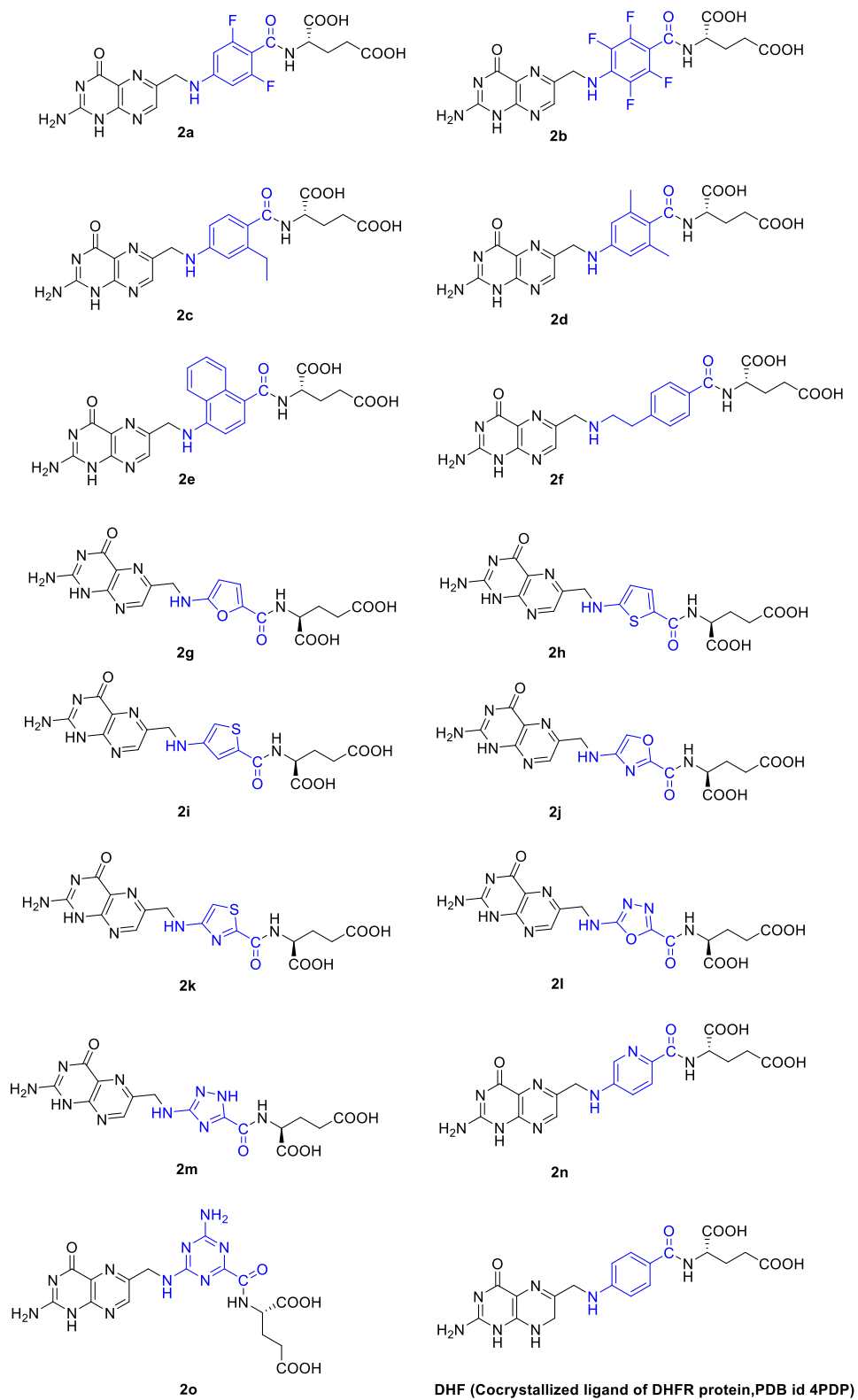


**Figure 5.** Designed structure of DHFR inhibitors **2a–o**

**Table 1.** Molecular docking score of designed DHFR inhibitors **2** with co-crystallized ligand, DHF

| DHFR inhibitors | MolDock Score |
|-----------------|---------------|
| DHF             | -161.573      |
| <b>2a</b>       | -159.466      |
| <b>2b</b>       | -107.23       |
| <b>2c</b>       | -133.434      |
| <b>2d</b>       | -126.051      |
| <b>2e</b>       | -147.605      |
| <b>2f</b>       | -142.448      |
| <b>2g</b>       | -143.765      |
| <b>2h</b>       | -149.564      |
| <b>2i</b>       | -154.126      |
| <b>2j</b>       | -140.773      |
| <b>2k</b>       | -154.556      |
| <b>2l</b>       | -135.06       |
| <b>2m</b>       | -146.632      |
| <b>2n</b>       | -134.724      |
| <b>2o</b>       | -142.92       |

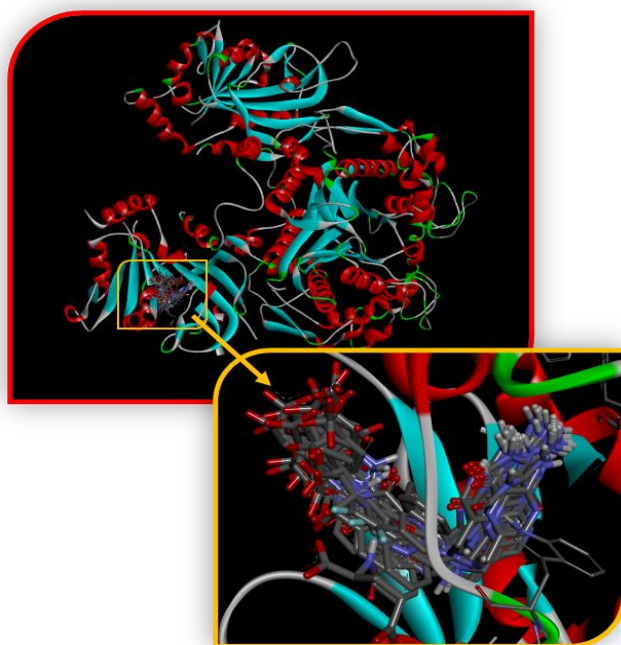


**Figure 6.** Superimposed orientation of newly designed DHFR inhibitors (**2a–o**) at the active site of DHFR protein (PBD ID 4DPD)

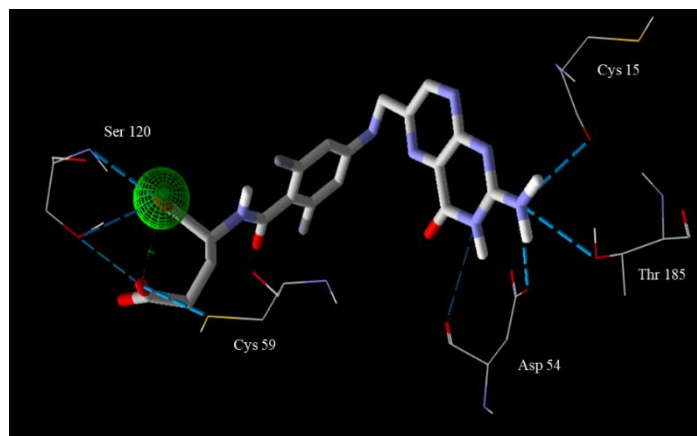


**Figure 7.** The H-bonding interactions of inhibitor **2a** at the active site of DHFR protein

## 4.2 DHPS Inhibitor

In the second study, the crystal structures of dihydropteroate synthetase (DHPS) (PDB ID 3TYE) was selected which is co-crystallised with sulfonamide-based inhibitor (ID-YTZ). Using similar protocol, the H-bonding interactions between the YTZ and amino acid residues of DHPS protein were analysed. Various sulfonamide and non-sulfonamide DHPS inhibitors were screened through molecular docking analysis and the best scoring inhibitors were selected for further study. The top scoring inhibitors **1a–d** and **11–20** are mentioned in figure 8. The molecular docking score of the designed inhibitors are mentioned in table 2. All the designed inhibitors interact at the active site in similar way as YTZ inhibitor. The superimposed orientations of all the ligands are mentioned in figure 9. Inhibitor **1b** score highest among all the inhibitors and hence H-bonding interactions of the inhibitor **1b** was evaluated in detail (Figure 10). All the designed inhibitors have shown significant interactions at the DHPS active site in *in silico* study. Synthesis of inhibitors **1a–d** and *in vitro* evaluation will be performed to validate the theoretical study.

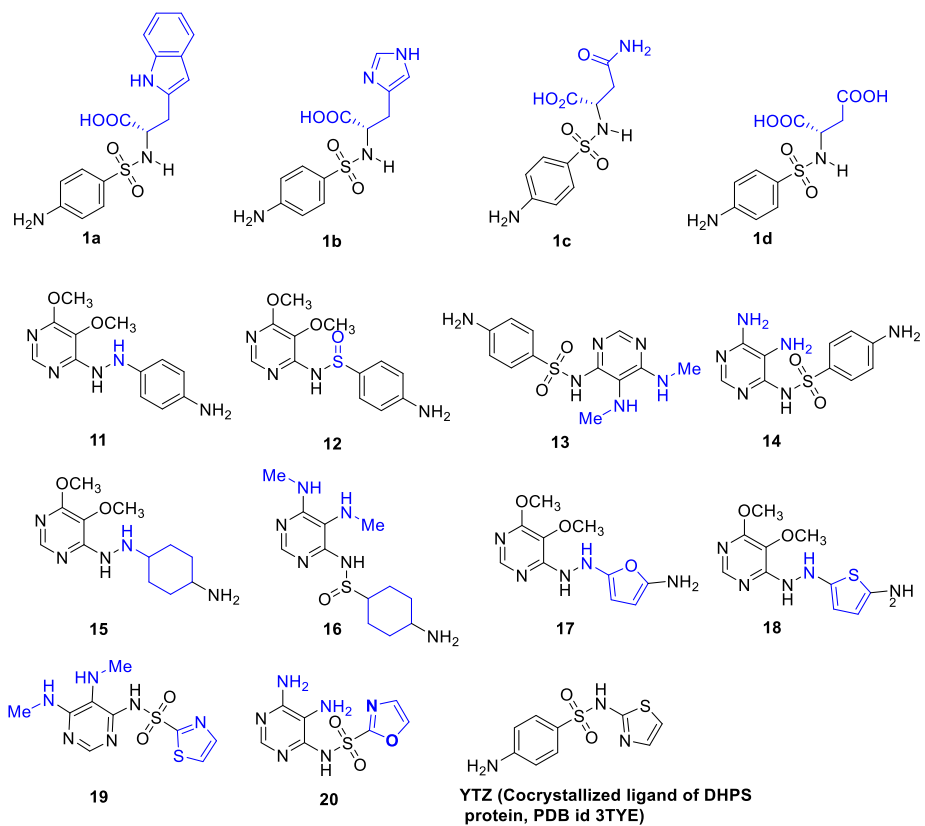


**Figure 8.** Designed structure of DHPS inhibitors **1a-d** and **11-20**

**Table 2.** Molecular docking score of designed DHPS inhibitors **1a–d** and **11–20** with co-crystallized ligand YTZ

| <b>Inhibitor</b> | <b>MolDock Score</b> |
|------------------|----------------------|
| YTZ              | -100.878             |
| <b>1a</b>        | -121.297             |
| <b>1b</b>        | -123.922             |
| <b>1c</b>        | -103.150             |
| <b>1d</b>        | -107.910             |
| <b>11</b>        | -66.7644             |
| <b>12</b>        | -82.3259             |
| <b>13</b>        | -83.5307             |
| <b>14</b>        | -84.7158             |
| <b>15</b>        | -69.1031             |
| <b>16</b>        | -72.7535             |
| <b>17</b>        | -78.4627             |
| <b>18</b>        | -80.7511             |
| <b>19</b>        | -82.2752             |
| <b>20</b>        | -82.9923             |

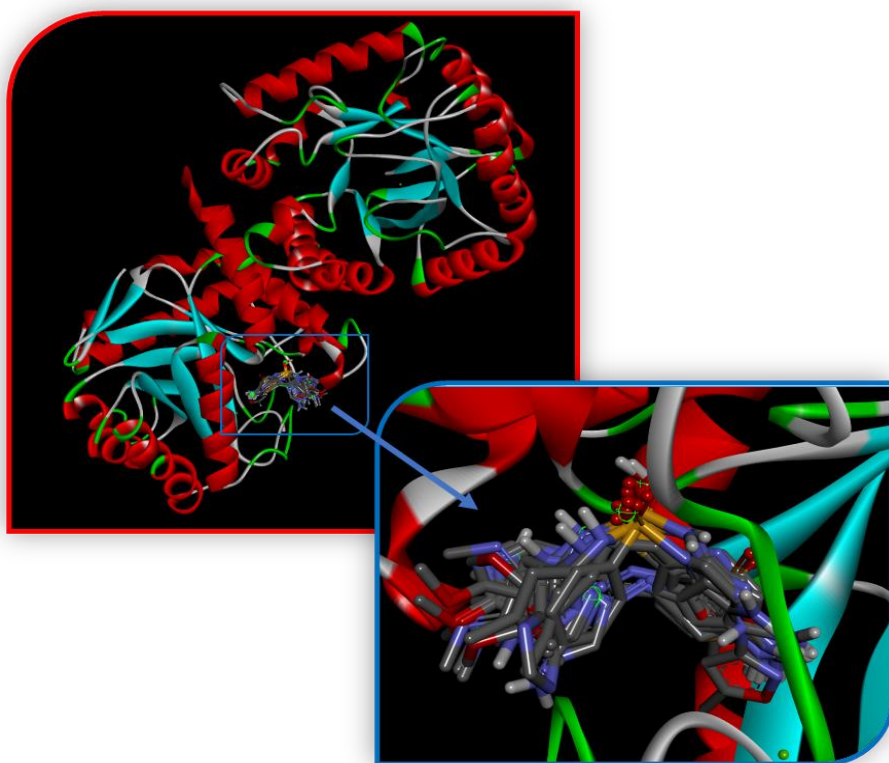


**Figure 9.** Superimposed orientation of newly designed DHPS inhibitors (**1a-d** and **11-20**) at the active site of DHPS protein (PBD ID 3TYE)

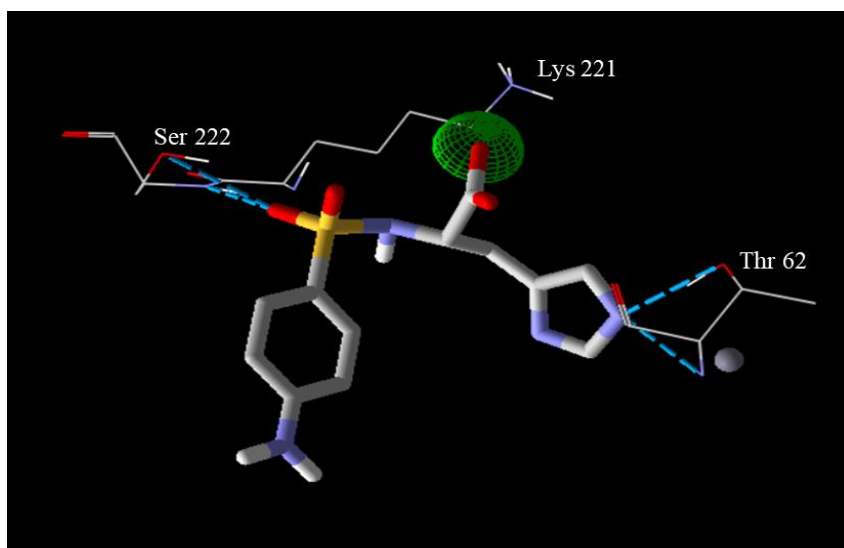


**Figure 10.** The H-bonding interactions of inhibitor **1b** at the active site of DHPS protein

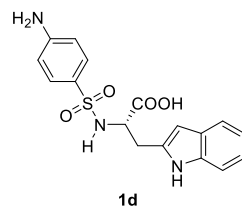
A total of four novel sulfonamides intermediates were synthesized in aqueous basic media by simple reaction of 4-nitrobenzenesulfonyl chloride and L-amino acids with continuous stirring. Compounds **5a–d** were synthesised from equimolar concentration of nitrobenzenesulfonyl chloride and a base. All the compounds except **5b** (41 %) were obtained in good yields.

The synthesized compounds were characterized by  $^1\text{H}$  NMR spectroscopy by dissolving in  $\text{CD}_3\text{OD}$ .  $^1\text{H}$  NMR of compound **5a** showed characteristic peaks of aromatic protons in the range of 7.45–7.77 ppm. A doublet of doublet at 3.23 ppm of protons of asymmetric center was obtained. The chemical shift values  $\delta$  in the range of 7.78–6.87 ppm was obtained for indolyl protons.

### 4.3 Retrosynthetic analysis of sulfonamide derivatives

A layout of retrosynthetic analysis is depicted in scheme 1. This is a linear retrosynthetic plan starting from moisture sensitive 4-nitrobenzene sulfonyl halides which can be converted to 4-aminobenzene sulfonamide by reacting with L-amino acids at a very low temperature and eventually reducing nitro group of 4-nitrobenzene sulfonyl halide by effective and efficient reduction method.

### 4.4 Synthesis of ((4-aminophenyl)sulfonyl)-L-tryptophan (**1d**)



As reported in the literature, the reaction of amino acids and sulfonyl chlorides using organic amine bases and organic solvents gave poor yield of the product. Schotten-Baumann conditions in organic solvents with aqueous basic solution also yield little product. Herein we used environment

friendly sulfonamide synthesis which was feasible at room temperature in green solvent water under pH control with  $\text{Na}_2\text{CO}_3$ .

We used a straightforward methodology for the synthesis of sulfonamide that can be used in large scale production. The direct sulfonamidation of amino acids was carried out to avoid tedious protection-deprotection steps. The hydrolysis of sulfonyl chloride is one of the side reactions and to minimize the competing hydrolysis reaction, the exposure of the sulfonyl chloride to the base and the solvent was minimized. To accomplish this method, water was used as a solvent and pH was maintained between 8 and 9 using  $\text{Na}_2\text{CO}_3$  to control the nucleophilic side reactions in water.

The reduction of nitrobenzenesulfonamides compounds under milder conditions in the presence of calcium chloride and iron powder in aqueous ethanol provided higher yields as reported in the literature. The short reaction time at relatively lower temperature makes it a suitable method for the reduction of nitrobenzenesulfonamides compounds.

### Conclusion and scope of work

The role of dihydrofolate reductase (DHFR) and dihydropteroate synthetase (DHPS) enzymes as remedial target in malaria treatment has been acknowledged for years. All the novel DHFR and DHPS inhibitors have heterocyclic moieties in their structures and using them in combination with other drugs may endow better antimalarial properties. This will be a promising approach for discovering novel antimalarial agents. The selective inhibition of protozoal enzymes is an achievable goal due to fundamental differences in protozoa and mammalian folate synthesis and utilization pathway. In this work, we have reported simple and efficient synthetic routes to synthesize chiral sulfonamides **1a–d**. We started the synthesis using L-amino acids as the chiral source and successfully prepared intermediates which can further furnish the final products, 4-aminobenzene sulfonamides.

## APPENDIX A

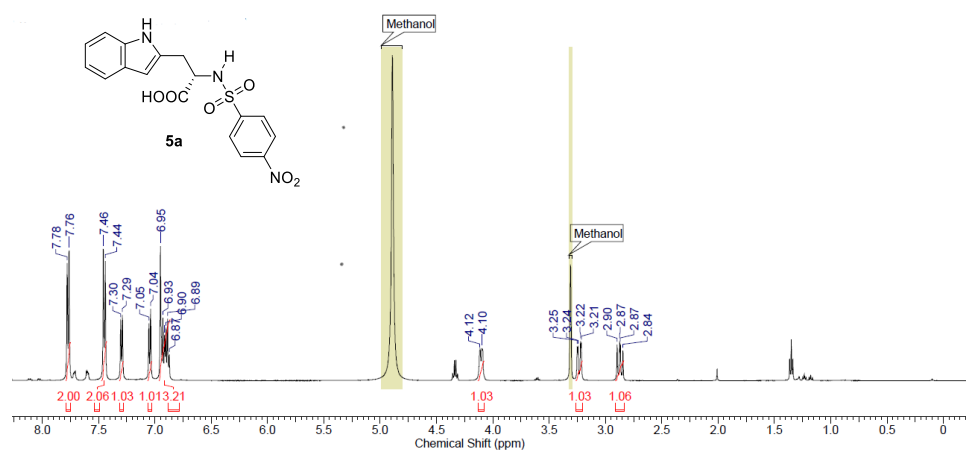


**Figure 11.** <sup>1</sup>H NMR spectrum of **5a** in methanol-*d*<sub>4</sub>

## References

1. World Malaria Report (2020), World Health Organization, Geneva.
2. Dondorp, A., Yeung, S., White, L., Nguon, C., Day, N.P.J., Socheat, D., Seidlein, L.V. (2010), Artemisinin resistance: Current status and scenarios for containment. *Nat. Rev. Microbiol.*, **8**, 272–280.
3. O’Brien, C., Henrich, P.P., Passi, N., Fidock, D.A. (2011), Recent clinical and molecular insights into emerging artemisinin resistance in *Plasmodium falciparum*. *Curr. Opin. Infect. Dis.*, **24**, 570–577.
4. Ivanetich, K.M., Santi, D.V. (1990), Bifunctional thymidylate synthase-dihydrofolate reductase in protozoa. *FASEB J.*, **4**, 1591–1597.
5. Yuvaniyama, J., Chitnumusub, P., Kamchonwongpaisan, S., Vanichtanankul, J., Sirawaraporn, W., Taylor, P., Walkinshaw, M.D., Yuthavong, Y. (2003), Insights into antifolate resistance from malarial DHFR-TS structures. *Nat. Struct. Mol. Biol.*, **10**, 327–365.
6. Kordus, S.L., Baughn, A.D. (2019), Revitalizing antifolates through understanding mechanism that govern susceptibility and resistance. *Med. Chem. Commun.*, **10**, 880–895.
7. Hevener, K.E., Yun, M., Qi, J., Kerr, I.D., Babaoglu, K., Hurdle, J.G., Balakrishna, K., White, S.W., Lee, R.E. (2011), Structural studies of pterin-based inhibitors of dihydropteroate synthase. *J. Med. Chem.* **53**, 166–177.
8. Nzila, A. (2006), Inhibitors of *de novo* folate enzymes in *Plasmodium falciparum*. *Elsevier*, **11**, 939–944.
9. Schnell, J.R., Dyson, H.J., Wright, P.E. (2004), Structure, dynamics and catalytic function of dihydrofolate reductase. *Annu. Rev. Biophys. Biomol. Struct.*, **33**, 119–140.

10. Fierke, C.A., Johnson, K.A., Benkovic, S.J. (1987), Construction and evaluation of the kinetic scheme associated with dihydrofolate reductase from *Escherichia coli*. *Biochemistry*, **26**, 4085–4092.
11. Williams, J.W., Morrison, J.F., Duggleby, R.G. (1979), The slow-binding and slow, tight-binding inhibition of enzyme-catalysed reactions. *Biochemistry*, **18**, 2567–2573.
12. Morrison, J.F., Walsh, C.T. (1988), The behavior and significance of slow-binding enzyme inhibitors. *Adv. Enzymol. Relat. Areas Mol. Biol.*, **61**, 201–301.
13. Babaoglu, K., Qi, J., Lee, R.E., White, S.W. (2004), Crystal structure of 7,8-dihydropteroate synthase from *Bacillus anthracis*: Mechanism and novel inhibitor design. *Structure*, **12**, 1705–1717.
14. Roland, S., Ferone, R., Harvey, R.J., Styles, V.L., Morrison, R.W. (1979), The characteristics and significance of sulfonamides as substrates for *Escherichia coli* dihydropteroate synthase. *J. Biol. Chem.*, **254**, 10337–10345.
15. Baca, A.M., Sirawaraporn, R., Turley, S., Sirawaraporn, W., Hol, W.G.J. (2000) Crystal structure of *Mycobacterium tuberculosis* 7,8-dihydropteroate synthase in complex with pterin monophosphate: New insight into the enzymatic mechanism and sulfa-drug action. *J. Mol. Biol.*, **302**, 1193–1212.
16. Levy, C., Minnis, D., Derrick, J.P. (2008), Dihydropteroate synthase from *Streptococcus pneumoniae*: Structure, ligand recognition and mechanism of sulfonamide resistance. *Biochem. J.*, **412**, 379–388.
17. Bourne, C. (2014) Utility of the biosynthetic folate pathway for targets in antimicrobial discovery. *Antibiotics*, **3**, 1–28.

18. Palmer, A.C., Kishony, R. (2014), Delayed commitment to evolutionary fate in antibiotic resistance fitness landscapes. *Nat. Commun.* **5**, 1–8.
19. Yun, M.K., Wu, Y., Li, Z., Zhao, Y., Waddell, M.B., Ferreira, A.M., Lee, R.E., Bashford, D., White, S.W. (2012), Catalysis and sulfa drug resistance in dihydropteroate synthase. *Science*, **335**, 1110–1114.
20. Chakraborty, S., Gruber, T., Barry, C.E., Boshoff, H.I., Rhee, K.Y. (2012) para-Aminosalicylic acid acts as an alternative substrate of folate metabolism in *Mycobacterium tuberculosis*. *Science*, **339**, 88–91.
21. Romano, K.P., Ali, A., Royer, W.E., Schiffer, C.A. (2010), Drug resistance against HCV NS3/4A inhibitors is defined by the balance of substrate recognition versus inhibitor binding. *Proc. Natl Acad. Sci. USA*, **107**, 20986–20991.